

## Magnetic Studies on Hexaiodorhenate(IV) Salts of Univalent Cations. Spin Canting and Magnetic Ordering in $K_2[ReI_6]$ with $T_c = 24$ K

Ricardo González,<sup>1a</sup> Raúl Chiozzone,<sup>1a</sup> Carlos Kremer,<sup>\*,1a</sup> Giovanni De Munno,<sup>\*,1b</sup> Francesco Nicolò,<sup>1c</sup> Francesc Lloret,<sup>1d</sup> Miguel Julve,<sup>1d</sup> and Juan Faus<sup>\*,1d</sup>

*Cátedra de Química Inorgánica, Facultad de Química de la Universidad de la República, Avda. General Flores 2124, CC 1157 Montevideo, Uruguay, Dipartimento di Chimica, Università degli Studi della Calabria, 87030 Arcavacata di Rende, Cosenza, Italy, Dipartimento di Chimica Inorganica, Chimica Analitica e Chimica Fisica, Università degli Studi di Messina, Via Salita Sperone 311-98166 Villaggio S. Agata, Messina, Italy, and Departamento de Química Inorgánica/ Instituto de Ciencia Molecular, Facultad de Química de la Universidad de Valencia, Dr. Moliner 50, 46100 Burjassot, Valencia, Spain*

Received September 3, 2002

The ionic salts of rhenium(IV) of formula  $(Cat)_2[ReI_6]$  with  $Cat = Li^+$  (**1**),  $Na^+$  (**2**),  $K^+$  (**3**),  $Rb^+$  (**4**),  $Cs^+$  (**5**),  $NH_4^+$  (**6**), and  $AsPh_4^+$  (**7**) [ $AsPh_4^+$  = tetraphenylarsonium cation] have been synthesized, and the structures of two of them (namely, **3** and **6**) were determined by single-crystal X-ray diffraction. **3** crystallizes in the monoclinic system, space group  $Pn$ , with  $a = 7.815(1)$  Å,  $b = 7.874(1)$  Å,  $c = 11.335(1)$  Å,  $\beta = 90.38(1)^\circ$ , and  $Z = 2$  whereas **6** crystallizes in the tetragonal system, space group  $P4/mnc$ , with  $a = 7.881(1)$  Å,  $b = 7.881(1)$  Å,  $c = 11.474(2)$  Å, and  $Z = 2$ . The structures of **3** and **6** are made up of discrete  $[ReI_6]^{2-}$  anions and  $K^+$  (**3**) or  $NH_4^+$  (**6**) cations held together by electrostatic forces (**3** and **6**) and  $N-H\cdots I$  hydrogen bonds (**6**). The rhenium(IV) cation in **3** and **6** is surrounded by six iodide ligands in an octahedral environment with the  $Re-I$  bond lengths varying in a very narrow range [2.704(3)–2.738(3) and 2.716(1)–2.722(2) Å for **3** and **6**, respectively]. The  $[ReI_6]^{2-}$  anions in **6** describe a tetragonally distorted body-centered cubic structure. In **3**, the arrangement of these units is similar but more distorted. The different arrangement of the anions in **3** and **6** accounts for the centrosymmetric (**6**) and non-centrosymmetric (**3**) structures observed. The magnetic properties of **1**–**7** were investigated in the temperature range 2.0–300 K. The magnetic behavior of **7** is that of a magnetically diluted Re(IV) complex with a large value of the zero-field splitting of the ground level ( $|2D| = 49.8$  cm<sup>-1</sup>) whereas those of **1**, **2**, and **4**–**6** are typical of antiferromagnetically coupled systems with susceptibility maxima at 28 (**1**), 27 (**2**), 21 (**4**), 16 (**5**), and 20 K (**6**). In the case of compound **3**, its magnetic behavior in the high-temperature range is parallel to that observed in the parent salts but below 24 K it is a weak ferromagnet with a canting angle of ca. 1.2°.

### Introduction

Hexahalorhenate(IV) salts are among the first examples of magnetic studies on rhenium(IV) complexes.<sup>2–5</sup> The

investigations of the magnetic properties of different ionic salts containing the  $[ReX_6]^{2-}$  anion ( $X = F, Cl, Br, \text{ or } I$ ) which were carried out by several research groups in the temperature range 80–300 K suggested the occurrence of large antiferromagnetic interactions between the paramagnetic Re(IV) centers (three unpaired electrons on each rhenium atom).<sup>2–9</sup> Figgis et al.<sup>8</sup> pointed out that the magnetic exchange in these systems depends on the tendency of the

\* Authors to whom correspondence should be addressed. E-mail: juan.faus@uv.es (J.F.); ckremer@bilbo.edu.uy (C.K.); demunno@unical.it (G.D.M.).

- (1) (a) Universidad de La República, Montevideo. (b) Università degli Studi della Calabria. (c) Università degli Studi di Messina. (d) Universidad de Valencia.
- (2) Schuth, W.; Klemm, W. *Z. Anorg. Allg. Chem.* **1934**, 220, 193.
- (3) Perakis, N. C. *R. Hebd. Seances Acad. Sci.* **1938**, 206, 1369.
- (4) Nelson, C. M.; Boyd, G. E.; Smith, W. T., Jr. *J. Am. Chem. Soc.* **1954**, 76, 348.
- (5) Figgis, B. N.; Lewis, J.; Nyholm, R. S.; Peacock, R. D. *Discuss. Faraday Soc.* **1958**, 26, 103.

- (6) Dalziel, J.; Gill, N. S.; Nyholm, R. S.; Peacock, R. D. *J. Chem. Soc.* **1958**, 4012.
- (7) Westland, A. D.; Bhiwandker, N. C. *Can. J. Chem.* **1961**, 39, 1284.
- (8) Figgis, B. N.; Lewis, J.; Mabbs, F. E. *J. Chem. Soc.* **1961**, 3138.
- (9) Spitsyn, V. I.; Zhironov, A. I.; Subbotin, M. Yu.; Kazin, P. E. *Russ. J. Inorg. Chem.* **1980**, 25, 556.

metal electrons to be transferred to the X ligand and on the X...X separation between the anions in the lattice. In this sense, they found that the antiferromagnetic interaction on different  $[\text{ReCl}_6]^{2-}$  salts can be related with the size of the cation, and that the magnitude of the magnetic coupling for the potassium and cesium salts of  $[\text{ReX}_6]^{2-}$  increases in the order  $\text{F} < \text{Cl} < \text{Br} < \text{I}$ , even when different crystal structures of the ionic salts are involved. For instance,  $\text{K}_2[\text{ReF}_6]$  has a  $\text{K}_2[\text{GeF}_6]$  type structure with slightly compressed  $[\text{ReF}_6]^{2-}$  octahedra,<sup>10</sup> and  $\text{K}_2[\text{ReCl}_6]$  and  $\text{K}_2[\text{ReBr}_6]$  exhibit regular octahedral structures of the  $\text{K}_2[\text{PtCl}_6]$  type,<sup>11</sup> whereas  $\text{K}_2[\text{ReI}_6]$  was found to be less symmetrical and its structure remains unsolved. An orthorhombic symmetry with four formula weights in the unit cell, in the possible space groups *Pm**cn*, *P2**1**cn*, *Pncn*, *Pbcn*, and *Pccn*, was proposed for  $\text{K}_2[\text{ReI}_6]$  on the basis of X-ray diffraction on powder samples of polycrystalline samples.<sup>12</sup> Some years later, and also on the basis of powder patterns, a different body-centered orthorhombic cell with two formula units was suggested for the structure of  $\text{K}_2[\text{ReI}_6]$ , even though some weak lines could be indexed when a related monoclinic cell containing four formula weights was used.<sup>6</sup>

Antiferromagnetic interactions were also observed for the  $\text{RNH}_3^+$  and  $\text{R}_2\text{NH}_2^+$  salts (R = methyl) of  $[\text{ReCl}_6]^{2-}$  and  $[\text{ReBr}_6]^{2-}$ .<sup>13,14</sup> However, the thermal variation of the magnetic susceptibility of the corresponding  $\text{R}_3\text{NH}^+$  and  $\text{R}_4\text{N}^+$  salts and that of the structurally characterized  $(\text{PPh}_4)_2[\text{ReCl}_6] \cdot 2\text{MeCN}$  ( $\text{PPh}_4^+$  = tetraphenylphosphonium cation) compound<sup>15</sup> were not satisfactorily explained.

Heat capacity measurements at low temperatures have shown typical  $\lambda$ -type anomalies at 11.9 K for  $\text{K}_2[\text{ReCl}_6]$ <sup>16</sup> and 15.2 K for  $\text{K}_2[\text{ReBr}_6]$ ,<sup>17</sup> which are associated with a cooperative-type transition to an antiferromagnetic ordered state.<sup>18</sup> An additional second-order transition for  $\text{K}_2[\text{ReCl}_6]$  at 76 K<sup>18</sup> coincides with a structural change to a cubic space group of lower symmetry.<sup>19</sup> The Néel temperatures were found to be 12.4 K for  $\text{K}_2[\text{ReCl}_6]$  and 15.3 K for  $\text{K}_2[\text{ReBr}_6]$ .

In a recent paper, we reported the temperature dependence of magnetic susceptibility of the magnetically diluted tetrabutylammonium and tetraphenylarsonium salts of  $[\text{ReCl}_6]^{2-}$ .<sup>20</sup> Their magnetic properties could be interpreted on the basis of zero-field splitting effects (*D*) originated on the combined action of the second-order spin-orbit coupling and a distorted octahedral ligand field on the  $^4\text{A}_{2g}$  ground state for a  $d^3$  ion. As the size of the cation increases, the intermo-

lecular chloro-chloro distance also increases and a weaker AF coupling is to be expected, so the ZFS effects became uppermost important. *2D* values of 18 and 26  $\text{cm}^{-1}$  were found for the tetrabutylammonium and tetraphenylarsonium derivatives, respectively ( $|2D|$  being the energy gap between the two Kramers doublets  $|\pm 3/2\rangle$  and  $|\pm 1/2\rangle$ ). This remarkable magnetic anisotropy can be understood by having in mind the large value of the spin-orbit coupling parameter ( $\lambda$  ca. 750  $\text{cm}^{-1}$  for  $[\text{ReCl}_6]^{2-}$  after reduction by covalency effects), and it was clearly present in the Re(IV) complexes that we investigated.<sup>20,21</sup>

The large degree of spin delocalization on the ligands is an important characteristic found in rhenium(IV) species, and it accounts for the intensity of the magnetic interactions observed between the Re(IV) centers at large distances. Polarized neutron diffraction experiments on neutral tetrachlorobis(*N*-phenylacetamide)rhenium(IV) showed that a significantly high amount of the spin of the system is covalent-delocalized away from the rhenium to ligands.<sup>22</sup> Density functional theory calculations of spin densities on the  $[\text{ReCl}_4(\text{ox})]^{2-}$  ion (ox = oxalate) also reveal a significant spin delocalization on the atoms of the coordination sphere of the rhenium atom.<sup>20</sup> Having in mind the variation in the covalent character of the rhenium-halogen bonds and the so expected increase of spin delocalization in the X ligands when going from X = F to X = I, we prepared the ionic Re(IV) salts of formula  $(\text{Cat})_2[\text{ReI}_6]$  with  $\text{Cat}^+ = \text{Li}^+$  (**1**),  $\text{Na}^+$  (**2**),  $\text{K}^+$  (**3**),  $\text{Rb}^+$  (**4**),  $\text{Cs}^+$  (**5**),  $\text{NH}_4^+$  (**6**), and  $\text{AsPh}_4^+$  (**7**) [ $\text{AsPh}_4^+$  = tetraphenylarsonium cation], investigated their magnetic properties as a function of the temperature, and determined the crystal structures of **3** and **6**. These magnetostructural results are presented here.

## Experimental Section

**Materials.** All reagents were purchased from commercial sources and used as received. Hexaiodorhenate(IV) salts were obtained by using a previously reported method<sup>23,24</sup> with slight modifications, which are detailed hereunder.

**Synthesis of the Complexes.  $\text{Li}_2[\text{ReI}_6]$  (**1**).**  $\text{HReO}_4$ , 60% (0.6 mL, 3.1 mmol), was added to a solution containing 2.9 g of LiI (21.7 mmol) in 15 mL of 47% HI. The mixture was stirred at 70 °C for 1 h, resulting in a dark solution. The volume of the solution was reduced to 2 mL by gentle evaporation at 35 °C. **1** separates as black crystals, which were filtered on a sintered glass funnel and dried at 70 °C for 1 h. Yield: 45–50%.

**$\text{Na}_2[\text{ReI}_6]$  (**2**).**  $\text{NaReO}_4$  (0.8 g, 2.9 mmol) and 2.2 g of NaI (14.7 mmol) were dissolved in 15 mL of 47% HI. The solution was stirred at 70 °C for 1 h. The volume of the resulting dark solution was reduced to 2 mL by gentle evaporation at 35 °C. **2** separates as black crystals, which were filtered on a sintered glass funnel and dried at 70 °C for 1 h. Yield: 55–60%.

- (10) Clark, G. R.; Russel, D. R. *Acta Crystallogr., Sect. B* **1978**, *34*, 894.  
 (11) Conner, K. A.; Walton, R. A. In *Comprehensive Coordination Chemistry*; Wilkinson, G., Gillard, R. D., McCleverty, J. A., Eds.; Pergamon Press: New York, 1987; Vol. 4, p 172.  
 (12) Morrow, J. C. *J. Phys. Chem.* **1956**, *60*, 19.  
 (13) Mrozinski, J. *Bull. Acad. Pol. Chim.* **1978**, *26*, 789.  
 (14) Mrozinski, J. *Bull. Acad. Pol. Chim.* **1980**, *28*, 559.  
 (15) Malecka, J.; Jäger, L.; Wagner, Ch.; Mrozinski, J. *Pol. J. Chem.* **1998**, *72*, 1879.  
 (16) Busey, R. H.; Dearman, H. H.; Bevan, R. B., Jr. *J. Phys. Chem.* **1962**, *66*, 82.  
 (17) Busey, R. H.; Bevan, R. B., Jr.; Gilbert, R. A. *J. Phys. Chem.* **1965**, *69*, 3471.  
 (18) Busey, R. H.; Sonder, E. *J. Chem. Phys.* **1962**, *36*, 93.  
 (19) Smith, H. G.; Bacon, G. E. *J. Appl. Phys.* **1966**, *37*, 979.  
 (20) Chiozzzone, R.; González, R.; Kremer, C.; De Munno, G.; Cano, J.; Lloret, F.; Julve, M.; Faus, J. *Inorg. Chem.* **1999**, *38*, 4745.

- (21) Chiozzzone, R.; González, R.; Kremer, C.; Armentano, D.; De Munno, G.; Cano, J.; Lloret, F.; Julve, M.; Faus, J. *Inorg. Chem.* **2001**, *40*, 4242.  
 (22) (a) Reynolds, P. A.; Moubaraki, B.; Murray, K. S.; Cable, J. W.; Engelhardt, L. M.; Figgis, B. N. *J. Chem. Soc., Dalton Trans.* **1997**, 263. (b) Reynolds, P. A.; Figgis, B. N.; Martin y Marero, D. *J. Chem. Soc., Dalton Trans.* **1999**, 945.  
 (23) Briscoe, H. V. A.; Robinson, P. L.; Rudge, A. J. *J. Chem. Soc.* **1931**, 3218.  
 (24) Chakravorti, M. C.; Gangopadhyay, T. *Inorganic Synthesis*; Ginsberg, A. P., Ed.; Wiley: New York, 1990; Vol. 27, p 294.

**K<sub>2</sub>[ReI<sub>6</sub>] (3).** KReO<sub>4</sub> (0.5 g, 1.7 mmol) and 1.5 g of KI (9.0 mmol) were dissolved in 15 mL of 47% HI. The solution was stirred at 70 °C for 1 h. The dark violet solution was allowed to stand at 2 °C for half an hour. **3** separates as black crystals, which were filtered on a sintered glass funnel and dried at 70 °C for 1 h. Yield: 70–80%. X-ray quality crystals of **3** were obtained by slow evaporation at room temperature of a solution of this compound in 47% HI.

**Rb<sub>2</sub>[ReI<sub>6</sub>] (4).** This complex was prepared as **3**, but using 465 mg of NH<sub>4</sub>ReO<sub>4</sub> (1.7 mmol), 1.6 g of RbI (7.5 mmol), and 20 mL of 47% HI. Yield: 90–95%.

**Cs<sub>2</sub>[ReI<sub>6</sub>] (5).** This complex was prepared as **3**, but using 465 mg of NH<sub>4</sub>ReO<sub>4</sub> (1.7 mmol), 2.25 g of CsI (8.7 mmol), and 20 mL of 47% HI. Yield: 90–95%.

**(NH<sub>4</sub>)<sub>2</sub>[ReI<sub>6</sub>] (6).** This complex was prepared as **3**, but using 465 mg of NH<sub>4</sub>ReO<sub>4</sub> (1.7 mmol), 1.3 g of NH<sub>4</sub>I (9.0 mmol), and 15 mL of 47% HI. Yield: 70–80%. Suitable crystals for X-ray diffraction were obtained by the same procedure used for **3**. Anal. Calcd for H<sub>8</sub>N<sub>2</sub>I<sub>6</sub>Re (**6**): N, 2.8; H, 0.8. Found: N, 2.9; H, 0.9.

**(AsPh<sub>4</sub>)<sub>2</sub>[ReI<sub>6</sub>] (7).** AsPh<sub>4</sub>Cl (81 mg, 0.19 mmol) dissolved in the minimum amount of methanol was added dropwise to a solution containing 100 mg (97.5 mmol) of **3** in 15 mL of 47% HI. The brown solid formed was filtered and washed with 0.5 M HI (2 × 2 mL), 2-propanol (2 × 2 mL), and diethyl ether (2 × 2 mL). Yield: 80%. Anal. Calcd for C<sub>48</sub>H<sub>40</sub>As<sub>2</sub>I<sub>6</sub>Re (**7**): C, 33.5; H, 2.8. Found: C, 33.2; H, 2.0.

Values of 1:6 for Re:I (**1** and **6**) and of 2:1:6 for Cat:Re:I [Cat = Na (**2**), K (**3**), Rb (**4**), Cs (**5**), and As (**7**)] molar ratios were determined by electron probe X-ray microanalysis at the Servicio Interdepartamental de Investigación de la Universitat de València. The lack of water molecules, ReO<sub>4</sub><sup>-</sup>, ReO<sub>2</sub>, and oxorhenium(V) impurities in **1–7** was checked by IR spectroscopy.

**Physical Techniques.** The IR spectra of **1–7** (CsI pellets) were recorded with a Bomen MB-102 FTIR spectrometer. Elemental analysis (C, H, N) was carried out on a Carlo Erba model 1108 elemental analyzer. Magnetic susceptibility measurements (2.0–300 K) were carried out with a Quantum Design SQUID magnetometer under an applied magnetic field of 1 T at high temperatures and only 100 G at low temperatures to avoid any problem of magnetic saturation. The device was calibrated with (NH<sub>4</sub>)<sub>2</sub>Mn(SO<sub>4</sub>)<sub>2</sub>·6H<sub>2</sub>O. The corrections for the diamagnetism were estimated from Pascal constants.

**X-ray Data Collection and Structure Refinement.** Crystals of dimensions 0.35 × 0.33 × 0.30 (**3**) and 0.31 × 0.22 × 0.26 mm (**6**) were mounted on a Bruker P4 automatic four-circle diffractometer and used for data collection. Diffraction data were collected at room temperature by using graphite-monochromated Mo K $\alpha$  radiation ( $\lambda = 0.71073$  Å) with the  $\omega$ -2 $\theta$  scan method. The unit cell parameters were determined from least-squares refinement of the setting angles of 25 reflections in the 2 $\theta$  range of 15–30°. Information concerning crystallographic data collection and structure refinements is summarized in Table 1. Examination of two standard reflections monitored after every 98 reflections showed no sign of crystal deterioration. Both data sets were corrected for Lorentz–polarization effects while  $\psi$ -scan absorption correction<sup>25</sup> was applied only for compound **3**. The systematic absence analysis on reflections for **3** reveals the  $P2_1/n$  symmetry. Nevertheless, no resolution was possible assuming this spatial group. On the contrary, resolution and refinement were obtained in  $P2_1$  and  $Pn$ , but the second one was better and for this reason it was assumed as the

**Table 1.** Summary of Crystal Data<sup>a</sup> for K<sub>2</sub>[ReI<sub>6</sub>] (**3**) and (NH<sub>4</sub>)<sub>2</sub>[ReI<sub>6</sub>] (**6**)

	<b>3</b>	<b>6</b>
chem formula	I <sub>6</sub> K <sub>2</sub> Re	H <sub>8</sub> I <sub>6</sub> N <sub>2</sub> Re
<i>M</i>	1025.8	983.68
cryst syst	<i>Pn</i>	<i>P4/mmc</i>
space group	monoclinic	tetragonal
<i>a</i> , Å	7.815(1)	7.881(1)
<i>b</i> , Å	7.874(1)	7.881(1)
<i>c</i> , Å	11.335(1)	11.474(2)
$\beta$ , deg	90.38(1)	90
<i>V</i> , Å <sup>3</sup>	697.4(1)	712.6(2)
<i>D<sub>c</sub></i> , g cm <sup>-3</sup>	4.885	4.584
<i>F</i> (000)	862	830
$\mu$ (Mo K $\alpha$ ), cm <sup>-1</sup>	22.53	21.48
reflins collected/obsd	2060/1526	1277/340
<i>R</i> <sup>b</sup>	0.068	0.044
<i>R<sub>w</sub></i> <sup>c</sup>	0.180	0.108
<i>S</i> <sup>d</sup>	1.036	1.005

<sup>a</sup> Details in common:  $T = 296(2)$  K,  $Z = 2$ , and  $I > 3\sigma(I)$ . <sup>b</sup>  $R = \sum(|F_o| - |F_c|)/\sum|F_o|$ . <sup>c</sup>  $R_w = wR2 = \{\sum[w(F_o^2 - F_c^2)^2]/\sum[w(F_o^2)^2]\}^{1/2}$ . <sup>d</sup> GOF =  $\{\sum[w(F_o^2 - F_c^2)/(N_o - N_p)]\}^{1/2}$ .

**Table 2.** Bond Distances (Å) and Bond Angles (deg) for Compound **3**<sup>a</sup>

Distances			
Re–I(1)	2.726(4)	Re–I(4)	2.720(4)
Re–I(2)	2.720(3)	Re–I(5)	2.738(3)
Re–I(3)	2.716(4)	Re–I(6)	2.704(4)
Angles			
I(1)–Re–I(2)	90.6(1)	I(2)–Re–I(6)	91.2(1)
I(1)–Re–I(3)	177.9(1)	I(3)–Re–I(4)	89.3(1)
I(1)–Re–I(4)	89.1(1)	I(3)–Re–I(5)	89.7(1)
I(1)–Re–I(5)	88.9(1)	I(3)–Re–I(6)	91.8(1)
I(1)–Re–I(6)	89.5(1)	I(4)–Re–I(5)	87.9(1)
I(2)–Re–I(3)	91.0(1)	I(4)–Re–I(6)	91.0(1)
I(2)–Re–I(4)	177.8(1)	I(5)–Re–I(6)	178.1(1)
I(2)–Re–I(5)	89.9(1)		

<sup>a</sup> Estimated standard deviations in the last significant digits are given in parentheses.

right spatial group with a pseudo center of symmetry. The structures of **3** and **6** were solved by standard Patterson methods and subsequently completed by Fourier recycling. Each refinement was performed by using full-matrix least-squares techniques on all  $F^2$  data. All non-hydrogen atoms were refined anisotropically. The disordered NH<sub>4</sub><sup>+</sup> cation of **6** has been treated as a “rigid body” refinement of the idealized tetrahedron, resulting in an overlap of four orientations by symmetry requirements. The residual maxima and minima in the final Fourier-difference maps were 3.30 and  $-4.86$  e Å<sup>-3</sup> for **3** and 1.54 and  $-3.71$  e Å<sup>-3</sup> for **6** (the first four residual maxima of **3** are near the rhenium atom). Solutions and refinements were performed with the SHELX NT system.<sup>26</sup> The final geometrical calculations were carried out with the PARST program.<sup>27</sup> The graphical manipulations were performed using the XP utility of the SHELX NT system. The interatomic bond lengths and angles for **3** and **6** are given in Tables 2 and 3, respectively.

## Results and Discussion

**Description of the Structures of K<sub>2</sub>[ReI<sub>6</sub>] (3) and (NH<sub>4</sub>)<sub>2</sub>[ReI<sub>6</sub>] (6).** The structure of compounds **3** and **6** is made up of [ReI<sub>6</sub>]<sup>2-</sup> anions (Figure 1) and K<sup>+</sup> (**3**) or NH<sub>4</sub><sup>+</sup> (**6**) cations which are held together by electrostatic forces. Hydrogen bonds involving the ammonium cations and iodide

(25) North, A. C. T.; Philips, D. C.; Mathews, F. S. *Acta Crystallogr., Sect. A* **1968**, *24*, 351.

(26) SHELX NT, version 5.10; Bruker Analytical X-Ray Systems: Madison, WI, 1998.

(27) Nardelli, M. *J. Appl. Crystallogr.* **1995**, *28*, 659.

**Table 3.** Bond Distances (Å) and Bond Angles (deg) for Compound **6**<sup>a,b</sup>

Distances			
Re–I(1)	2.722(2)	Re–I(2)	2.716(1)
Angles			
I(1)–Re–I(2)	90.0	I(1)–Re–I(1a)	180.0

<sup>a</sup> Estimated standard deviations in the last significant digits are given in parentheses. <sup>b</sup> Symmetry code: (a) = 3 – x, –y, –z + 1.

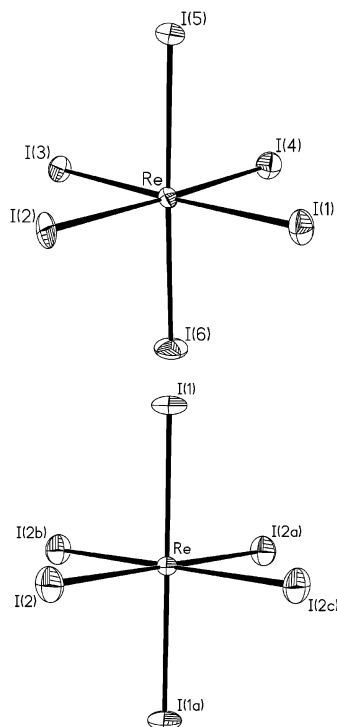


**Figure 1.** Perspective drawing of the  $[\text{ReI}_6]^{2-}$  anion in **3** (top) and **6** (bottom) showing the atom numbering. Thermal ellipsoids are drawn at the 30% probability level.

ligands in **6** [ $\text{N}\cdots\text{I}$  distances ranging from 3.778(1) to 3.943(1) Å] contribute to the stabilization of the structure.

In compound **6**, the anions are formed by six iodide ligands bound to a rhenium(IV) cation in a regular octahedral geometry, in which the Re–I(1) and Re–I(2) bond lengths are practically identical [2.722(2) and 2.716(1) Å, respectively] and the relative angles are 90° and 180°. These anions also occur in **3**, but they are slightly distorted: assuming that I(5) and I(6) occupy the axial positions and that I(1), I(2), I(3), and I(4) lie in the equatorial ones, the equatorial Re–I bonds are almost equal [average value 2.720 Å] whereas the axial ones are somewhat shorter [2.704(3) Å for Re–I(6)] or longer [2.738(3) Å for Re–I(5)]. The  $[\text{ReI}_6]^{2-}$  anions are oriented in such a way that their Re–I(5) and Re–I(1) bonds for **3** and **6**, respectively, lie approximately (**3**) or exactly (**6**) along the crystallographic  $z$  axis (Figure 2). All the  $[\text{ReI}_6]^{2-}$  anions in an  $xy$  plane have the same orientation in both compounds. However, in the case of **3**, adjacent  $xy$  planes contain anions showing different orientation. These planes are shifted in **3** and **6**, so that every  $[\text{ReI}_6]^{2-}$  anion is at the center of a parallelepiped formed by eight similar anions (Figure 3).

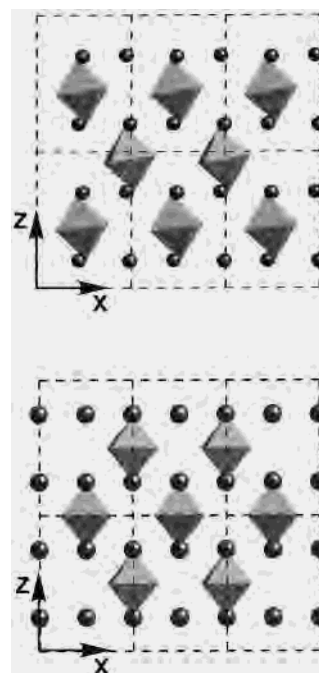


**Figure 2.** Projection of the structure of **3** (top) and **6** (bottom) along the  $y$  axis showing the relative arrangement of the  $[\text{ReI}_6]^{2-}$  units (octahedra) and potassium (top) and ammonium (bottom) cations (circles).

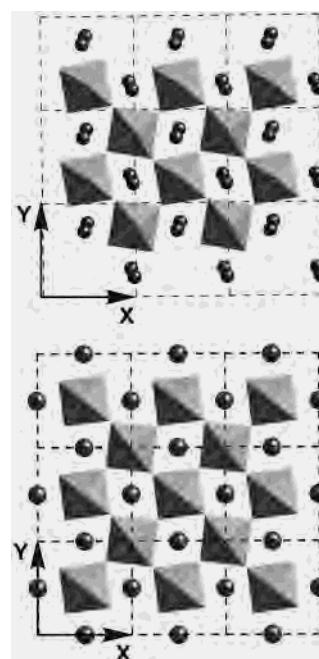


**Figure 3.** Projection of the structure of **3** (top) and **6** (bottom) along the  $z$  axis showing the tetragonally distorted body-centered cubic arrangement of the  $[\text{ReI}_6]^{2-}$  units (octahedra) and the position of the potassium (top) and ammonium (bottom) cations (circles).

In compound **3**, the relative  $\text{I}\cdots\text{I}$  distances are 4.167(5), 4.068(4), 4.218(4), and 4.279(5) Å for I(6) $\cdots$ I(1a), I(6) $\cdots$ I(2b), I(6) $\cdots$ I(3c), and I(6) $\cdots$ I(4d), and 4.287(4), 4.263(49), 4.120(4), and 4.151(4) Å for I(5e) $\cdots$ I(1a), I(5e) $\cdots$ I(2b), I(5e) $\cdots$ I(3c), and I(5e) $\cdots$ I(4d), respectively (Figure 4, top) [symmetry codes: (a) 0.5 + x, 1 – y, –0.5 + z; (b) –0.5 + x, 1 – y, –0.5 + z; (c) –0.5 + x, –y, –0.5 + z; (d) 0.5 + x, –y, –0.5 + z; (e) x, y, –1 + z]. They are comparable with

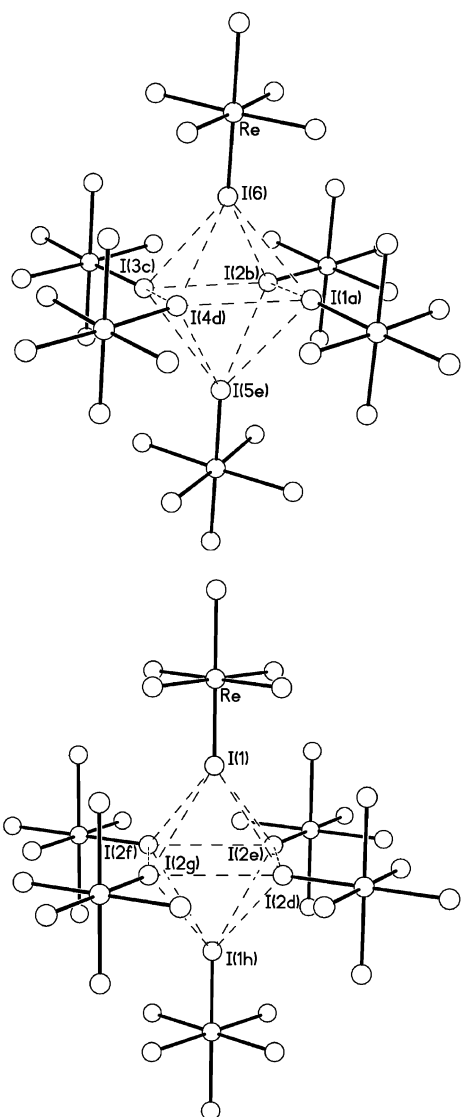


**Figure 4.** A view of the shortest I⋯I contacts (broken lines) among the  $[\text{ReI}_6]^{2-}$  anionic units in **3** (top) and **6** (bottom).

the I⋯I separations in the  $xy$  plane, which are 4.128(5), 4.163(4), 4.093(4), and 4.167(5) Å for I(1a)⋯I(2b), I(1a)⋯I(4d), I(2b)⋯I(3c), and I(3c)⋯I(4d), respectively. The corresponding ones for **6** are more regular: 4.179(2) Å for I(1)⋯I(2d), I(1)⋯I(2e), I(1)⋯I(2f), and I(1)⋯I(2g) and also for I(1h)⋯I(2d), I(1f)⋯I(2e), I(1f)⋯I(2f), and I(1f)⋯I(2g) (Figure 4, bottom); 4.094(2) Å for I(2d)⋯I(2e), I(2e)⋯I(2f), I(2f)⋯I(2g), and I(2g)⋯I(2d) in the  $xy$  plane [symmetry codes: (d)  $0.5 - x, 0.5 + y, 0.5 - z$ ; (e)  $-0.5 - x, 0.5 - y, 0.5 - z$ ; (f)  $-0.5 + x, -0.5 - y, 0.5 - z$ ; (g)  $-0.5 + x, 0.5 + y, 0.5 - z$ ; (h)  $x, y, -z$ ].

**Magnetic Properties.** In this section, (i) we will present first the magnetic properties the mononuclear compound **7** in order to visualize the magnetic behavior of the  $[\text{ReI}_6]^{2-}$  unit (the bulky  $\text{AsPh}_4^+$  most likely maximizes the I⋯I separation between adjacent anions and minimizes the interanion magnetic interaction) which is also present in compounds **1–6**. (ii) In a second step, the magnetic properties of the series **1, 2, 4, 5**, and **6** will be discussed together given that they exhibit a similar antiferromagnetic coupling

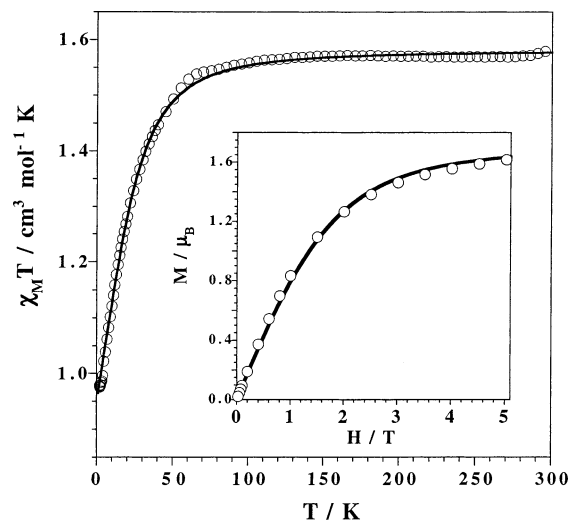


**Figure 5.** Thermal variation of the  $\chi_M T$  product for compound **7**: (O) experimental data; (—) best fit through eqs 1–5 from ref 20. The inset shows the magnetization curve for **7** at 2 K: (O) experimental data; (—) best fit through the Brillouin function for a magnetically isolated spin quadruplet with  $g$  and  $|2D|$  as variable parameters (see text).

(susceptibility maxima in the temperature range 20–30 K). (iii) Finally, the original magnetic behavior of complex **3** (ferromagnetic ordering through spin canting), moved us to discuss its magnetic properties separately.

(i) The magnetic properties of compound **7** in the form of  $\chi_M T$  versus  $T$  ( $\chi_M$  being the molar magnetic susceptibility) are shown in Figure 5. At room temperature, the value of  $\chi_M T$  is close to  $1.6 \text{ cm}^3 \text{ mol}^{-1} \text{ K}$ . This value is as expected for a magnetically isolated mononuclear  $\text{Re(IV)}$  ( $S = 3/2$ ) complex with  $g = 1.8\text{--}1.9$  (see below and ref 20).  $\chi_M T$  for **7** remains practically constant upon cooling until 100 K. At lower temperatures, it decreases and tends to a finite value close to  $1 \text{ cm}^3 \text{ mol}^{-1} \text{ K}$  at 2 K. The magnetization ( $M$ ) plot of **7** as a function of the applied magnetic field ( $H$ ) at 2 K (inset of Figure 5) shows that the  $M$  increases with  $H$  and tends to a saturation value of  $1.6 \mu_B$  at 5 T. This magnetic behavior corresponds to that of a magnetically isolated mononuclear rhenium(IV) complex,<sup>20</sup> the bulky  $\text{AsPh}_4^+$  cation ensuring the magnetic dilution of the  $[\text{ReI}_6]^{2-}$  magnetic units. The decrease of  $\chi_M T$  for **7** at low temperatures is due to zero-field splitting effects. These effects account for the low value of the saturation magnetization too ( $M_S = 2.7 \mu_B$  for a  $S = 3/2$  ion with  $g = 1.8$ ). In fact, six-coordinated  $\text{Re(IV)}$  is a  $d^3$  type ion and, for such a case, the first excited state which arises from  $4F$  free-ion ground state is  $4T_{2g}$ . Under a tetragonal distortion, this excited state is split into  $4B_2$  and  $4E$  states. Under this pattern, the interaction of these two excited states with the quartet ground spin state leads to two Kramers doublets,  $|\pm 3/2\rangle$  and  $|\pm 1/2\rangle$ , which are separated by an energy gap of  $|2D|$  (zero-field splitting resulting from the combined action of the second-order spin–orbit interaction and the tetragonal crystal field). Assuming that this scheme can be applied to compound **7** [although the structure of this compound is unknown, the  $[\text{ReI}_6]^{2-}$  anion it contains could exhibit a tetragonal distortion as observed in the potassium derivative (compound **3**)], least-squares fitting of its magnetic data through the previously derived expression<sup>20</sup>

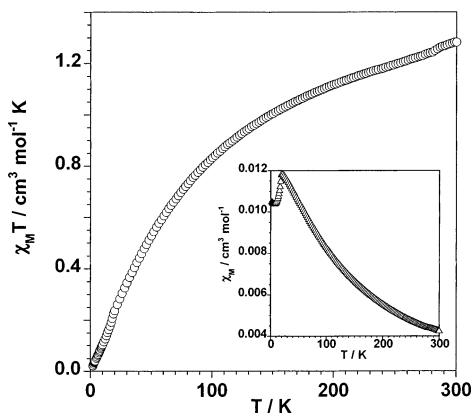


**Figure 6.** Thermal variation of the  $\chi_M T$  product (○) and  $\chi_M$  (Δ) for compound **6**.

leads to  $|2D| = 49.8 \text{ cm}^{-1}$  and  $g = 1.84$ . The calculated curve matches very well the magnetic data in the whole temperature range. The fact that the fit of the magnetization curve of **7** through the Brillouin function for a magnetically isolated  $S = 3/2$  with  $g$  and  $|2D|$  as variable parameters is also very satisfactory (see inset of Figure 5) with  $g = 1.84$  and  $|2D| = 48.6$  (values which are practically identical to those of the previous fit) provides additional support to the validity of our assumptions. The high value of the zero-field splitting for the Re(IV) ion in **7** contrasts with the lower values found for the first-row transition metal ions. The large value of the spin-orbit parameter ( $\lambda$ ) of the third-row transition elements [ $\lambda$  values of 90 and  $1100 \text{ cm}^{-1}$  for the  $d^3$  Cr(III) and Re(IV) single ions, respectively]<sup>8</sup> would account for this difference. Values of  $|2D|$  of 18, 26, and  $120 \text{ cm}^{-1}$  were found for the magnetically isolated Re(IV) mononuclear complexes (NBut<sub>4</sub>)<sub>2</sub>[ReCl<sub>6</sub>] (NBut<sub>4</sub><sup>+</sup> = tetrabutylammonium cation), (AsPh<sub>4</sub>)<sub>2</sub>[ReCl<sub>6</sub>], and (AsPh<sub>4</sub>)<sub>2</sub>[ReCl<sub>4</sub>(ox)] (ox = oxalate dianion), respectively.<sup>20</sup>

(ii) The  $\chi_M T$  versus  $T$  plots of **1**, **2**, and **4–6** are similar, and that of **6** is given in Figure 6 as an illustrative example. At room temperature,  $\chi_M T$  values vary between 1.4 and  $1.2 \text{ cm}^3 \text{ mol}^{-1} \text{ K}$ . These values are below that observed for **7**, suggesting that a significant antiferromagnetic interaction occurs in this series of compounds. Upon cooling, the values of  $\chi_M T$  quickly decrease, and they vanish at very low temperatures. The susceptibility curves show the occurrence of maxima at 28 (**1**), 27 (**2**), 21 (**4**), 16 (**5**), and 20 K (**6**, inset Figure 6). These features are characteristic of antiferromagnetically coupled systems and, given the ionic nature of the present family of compounds, would lead to three-dimensional antiferromagnetic ordering at temperatures slightly below those of the susceptibility maxima. The values of  $T_N$  nicely follow the size of the cation:  $T_N$  decreases as far as the size of the cation increases. Keeping in mind that the exchange interaction in this family of ionic salts involves the Re–I⋯I–Re pathway, the shorter I⋯I separation between the paramagnetic [ReI<sub>6</sub>]<sup>2-</sup> anions expected for smaller cations would account for this trend. Even when the size of the cations involved is very close (case of compounds **3** and **6**), the shortest I⋯I separation is somewhat different [4.068(4) (**3**) and 4.094(4) Å (**6**)]. The relative large spin

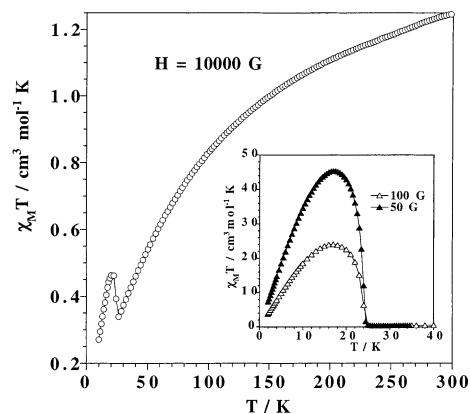


**Figure 7.** Thermal variation of the  $\chi_M T$  product for compound **3** under an applied magnetic field of 10000 G. The inset shows the thermal variation of  $\chi_M T$  in the low-temperature range and under magnetic fields of 100 and 50 G (the solid line is an eye-guide).

delocalization on the peripheral ligands in the compounds with third-row transition metal ions when compared with the compounds containing first-row transition cations, which was first suggested by Owen and Steven in 1953 on the basis of EPR measurements<sup>28</sup> and corroborated later by neutron diffraction measurements,<sup>22</sup> accounts for the relatively important through space magnetic interactions in this series. Recent DFT type calculations on the [Re(Cl<sub>4</sub>(ox))]<sup>2-</sup> anion also indicate a large spin delocalization on the peripheral ligands.<sup>20</sup> Most likely, the bulkier AsPh<sub>4</sub><sup>+</sup> cation in **7** increases the I⋯I separation and causes the magnetic dilution observed for this compound.

(iii) The magnetic properties of the potassium salt (compound **3**) in the form of a  $\chi_M T$  versus  $T$  plot is shown in Figure 7. The shape of the curve in the high-temperature range is similar to that observed in the previous compounds. At room temperature,  $\chi_M T$  is ca.  $1.24 \text{ cm}^3 \text{ mol}^{-1} \text{ K}$ . This value quickly decreases upon cooling until 25 K, where it exhibits an abrupt increase, and then it decreases with  $T$ . This increase is more pronounced at lower fields (see inset of Figure 7), where saturation effects are minimized. The variation of  $\chi_M T$  in the high-temperature range for **3** reveals that a relatively large antiferromagnetic coupling between the Re(IV) occurs. The abrupt increase of  $\chi_M T$  in the low-temperature region can be attributed to a spin canting. This spin canting in **3** is due to the great anisotropy of the Re(IV) ion and to the lack of inversion center in the structure [see Figure 3 (top)].<sup>29</sup>

FCM (field-cooled magnetization) of **3** under 100 and 50 G (Figure 8) shows the occurrence of magnetic ordering below 24 K. The magnetization saturates at a value of  $200 \text{ cm}^3 \text{ mol}^{-1} \text{ G}$  (at 100 G). This low value indicates the occurrence of a weak ferromagnetism. A maximum at 24 K is observed in the in-phase signal of the ac measurements on a polycrystalline sample of **3** (inset of Figure 8) under different frequency values. The magnetic hysteresis loops were performed at 1.9, 5, and 15 K (see Figure 9). A well-

(28) Owen, J.; Steven, K. *Nature* **1953**, *171*, 836.

(29) Bencini, A.; Gatteschi, D.; *Electron Paramagnetic Resonance of Exchange Coupled Systems*; Springer-Verlag: Berlin, 1990.

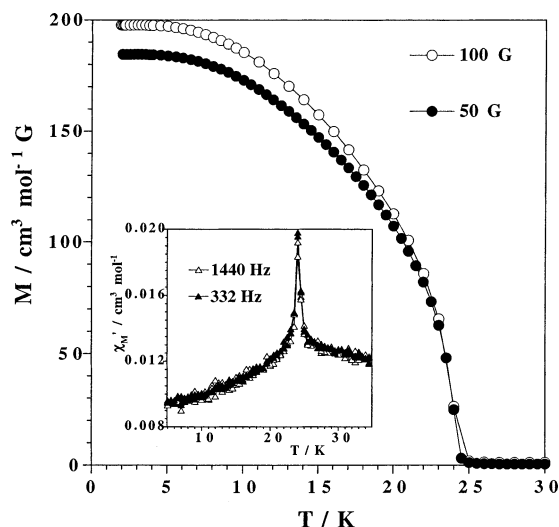


**Figure 8.** FCM for compound **3** at  $H = 100$  and  $50$  G. The inset shows the in-phase ac signal at two different frequency values.

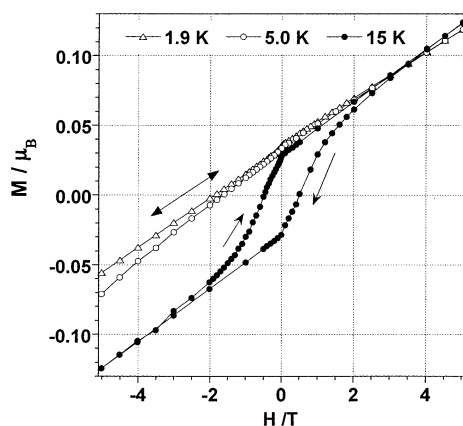


**Figure 9.** Hysteresis loops for **3** at 1.9, 5, and 15 K.

defined loop was obtained only at 15 K with values of the coercive field ( $H_c$ ) and remnant magnetization ( $M_r$ ) of 5000 G and  $0.028 \mu_B$ , respectively. The magnetization at the maximum available field (5 T) for this temperature is only  $0.12 \mu_B$ , and is far from the saturation value. This is in agreement with the presence of a weak ferromagnetism. At  $T < 15$  K, the value of  $H_c$  increases until ca. 2 T (1.9 K) whereas that of  $M_r$  are similar. However, it is not possible to complete the hysteresis loop at these low temperatures between  $+5$  and  $-5$  T. So, as shown in Figure 9, when moving from  $+5$  T to  $-5$  T and then coming back, the magnetization values follow the same path. Greater magnetic fields would be required to get a complete hysteresis loop. The evaluation of the canting angle ( $\alpha$ ) in **3** can be obtained

through eq 1,<sup>30</sup>

$$\sin \alpha = M_w / M_S \quad (1)$$

where  $M_w$  is the magnetization induced by a very weak magnetic field and  $M_S$  is the saturation magnetization. Although no saturation magnetization is obtained for **3**, a value of  $\alpha = 1.2^\circ$  can be roughly estimated by assuming that  $M_S = 1.6$  (value from compound **7**) and that  $M_w \approx M_r$  at 1.9 K ( $0.035 \mu_B$ ). This value lies within the range of those usually reported for systems exhibiting weak ferromagnetism.<sup>31</sup>

We would like to finish this contribution outlining the influence of the cation of the ionic salts  $(\text{Cat})_2[\text{ReI}_6]$  (**1–6**) on the magnetic properties. All these compounds exhibit through space antiferromagnetic coupling, the exchange pathway being  $\text{Re}-\text{I}\cdots\text{I}-\text{Re}$ . They are ionic salts that exhibit magnetic ordering through interionic interactions with relatively high  $T_N$  values. In the case of the potassium derivative (**3**), a weak ferromagnetism due to spin canting is observed. The structural knowledge of two members of this series, namely, the potassium (**3**) and ammonium derivatives (**6**), allows us to account for this peculiar magnetic behavior of **3**. Although the potassium and ammonium cations (ions with the same charge and very close size) usually afford isostructural compounds, this is not the present case given that compound **3** crystallizes in the monoclinic system, space group  $Pn$ , whereas **6** crystallizes in the tetragonal system, space group  $P4/mnc$ . The acentric character of the former spatial group would account for the spin canting observed in **3**. In near future, additional work using paramagnetic cations such as ferrocenium and organic radicals will be carried out aiming at enhancing the intermolecular interactions between the spin carriers and getting magnetic ordering at higher temperatures.

**Acknowledgment.** Financial support from the Training and Mobility Research Program from the European Union (TMR Contract ERBFMRXCT-980181), the Ministerio Español de Ciencia y Tecnología (Project BQU2001-2928), and the Italian Ministero dell'Università e della Ricerca Scientifica e Tecnologica is gratefully acknowledged. R.C. and R.G. are indebted to the European Union for a grant [ALFA Programme ALR/B7-3011/94.04-5.02273(9)].

**Supporting Information Available:** X-ray crystallographic files of compounds **3** and **6** in CIF format. This material is available free of charge via the Internet at <http://pubs.acs.org>.

IC020531J

(30) Kahn, O. *Molecular Magnetism*; VCH: New York, 1993.

(31) Carlin R. *Magnetochemistry*; Springer-Verlag: Berlin, 1986.